

## Photostimulated Generation of Defects and Surface Reactions on a Series of Wide Band Gap Metal-Oxide Solids

A. V. Emeline,<sup>†</sup> G. V. Kataeva,<sup>‡</sup> V. K. Ryabchuk,<sup>‡</sup> and N. Serpone<sup>\*,†</sup>

Department of Chemistry & Biochemistry, Concordia University, 1455 de Maisonneuve Boulevard West, Montréal (Québec), Canada H3G 1M8, and Department of Physics, University of St. Petersburg, Ulianovskaia 1, St. Petersburg, 198904 Russia

Received: February 23, 1999; In Final Form: June 19, 1999

The interconnection between photostimulated formation and destruction of defect centers (F- and V-type color centers) and surface photochemical reactions taking place on the surface has been examined for a series of 21 wide band gap metal-oxide specimens, which comprise insulators and semiconductors whose band-gap energies span the range from ca. 3 eV (ZnO, TiO<sub>2</sub>) to ca. 11 eV (BeO). Photostimulated post-adsorption of O<sub>2</sub> was seen for 9 of the 21 metal oxides tested. Three of these specimens, namely scandia (Sc<sub>2</sub>O<sub>3</sub>), zirconia (ZrO<sub>2</sub>), and normal spinel (MgAl<sub>2</sub>O<sub>4</sub>), were chosen for detailed study to establish that spectral sensitization of metal oxides by UV illumination is a generally occurring phenomenon which is carried over to photostimulated adsorption of molecules and to surface photochemical reactions. Results demonstrate that irradiation into the absorption bands of the color centers of the photocolored metal oxides leads to a red shift of the spectral limit of surface photoreactions. A simple mechanism is described quantitatively for the photocoloration and surface reactions. Quantum yields of photobleaching of color centers in vacuo and in the presence of H<sub>2</sub> and O<sub>2</sub> are reported for scandia and zirconia, together with the quantum yields of photoadsorption of H<sub>2</sub> and O<sub>2</sub> molecules.

### Introduction

Interaction of light with a solid/gas or a solid/liquid system has attracted much worldwide attention<sup>1–6</sup> in advancing fundamental scientific knowledge and numerous technological applications: e.g., optical and electronic devices, environmental remediation, and heterogeneous photochemistry and photocatalysis. Such interactions differ by which partner of the heterogeneous system absorbs photons. Absorption by molecules of the gas or liquid phase adsorbed on the solid's surface leads to several consequences, most notable being formation of excited states of adsorbed molecules, followed by (i) luminescence and energy and/or electron transfer along the layer of adsorbed molecules, or to molecules in the gas or liquid phase or to the bulk of the solid, and (ii) by secondary chemical processes. The second possibility is light absorption by the solid producing its own excited states: e.g. excitons, free charge carriers (electrons and holes), phonons, and others. Energy or charge transfer toward the surface may lead to surface chemical reactions with adsorbed molecules or with molecules in the gas or liquid phase diffusing toward the surface. Other decay channels for the solid's excited states are recombination of the charge carriers and the excitons resulting in photon evolution (radiative recombination, i.e., luminescence) or phonon emission (nonradiative recombination). Incomplete recombination of carriers and excitons leads to radiation-stimulated formation of defects in semiconductors and insulators.

Defect formation in metal-oxide specimens occurs by excitation of the electronic subsystem of the solids under irradiation by light of moderate photon energies in the range below the

impact displacement energy threshold (e.g., as might occur when specimens are irradiated with high-energy radiation) down to the band-gap energies  $E_{bg}$  of the solids, and perhaps even lower. For wide band gap ionic crystals, defect formation may occur by two fundamental pathways as a result of excitation of the electronic subsystem of crystals.<sup>7</sup> The decay of excitons into intrinsic ion vacancies and interstitials in regular lattices have been well established for alkali metal halides and other solids.<sup>8–10</sup> Two conditions favor this kind of defect formation: (i)  $E_{ex} > E_d$ , i.e., the exciton energy  $E_{ex}$  must exceed the energy  $E_d$  of defect (Fraenkel pair) formation (energy conservation law); and (ii)  $\tau_{ex} > \tau_{vib}$ , i.e., the lifetime of self-trapped excitons in a given regular lattice site,  $\tau_{ex}$ , must be longer than the period of lattice vibrations:  $\tau_{vib} \sim 10^{-12}–10^{-13}$  s (the momentum conservation law).<sup>11</sup> Formation of a Fraenkel pair defect as a primary product of the photoreaction in a regular lattice is equivalent to the photodissociation of free molecules. However, the decay of excitons into Fraenkel pairs, well-known in alkali metal halides, remains a contentious issue for wide band gap metal oxides,<sup>7</sup> primarily because of the failure of either one or both of conditions (i) and (ii) above.

A complex interconnection between surface photochemical processes and defect formation in solids is caused by common stages of photoexcitation and the participation of photoexcited electronic subsystems in both processes, which typically manifest themselves as an influence of the photoadsorption of molecules on the photocoloration of powdered solids.<sup>12–14</sup>

One result connected with photoinduced defects (color centers) is the spectral sensitization of solids in connection with the spectral limit of surface photoreactions. This spectral sensitization was originally observed on alkali metal halides by Ryabchuk and co-workers<sup>15</sup> with respect to the photostimulated adsorption of O<sub>2</sub> and CO<sub>2</sub>, which manifests itself as a red shift of the spectral limit of photoreactions.

\* Author to whom correspondence should be addressed at Concordia University. Fax: 514-848-2868. E-mail: serpone@vax2.concordia.ca.

<sup>†</sup> Concordia University.

<sup>‡</sup> University of St. Petersburg.

**TABLE 1: Summary of Data from Preliminary Tests of Metal-Oxide Specimens Examined for the Photostimulated Post-Adsorption of Oxygen**

metal oxide	$E_{bg}^a$ (eV)	$\Delta R_{vac}^b$ ( $10^{-3}$ )	$\delta R_{vac}^c$ ( $10^{-4}$ )	$\delta R_{O_2}^d$ ( $10^{-4}$ )	$(\delta R/\Delta R)_{vac}^e$	$dP/dt$ (PhA) <sup>f</sup> ( $10^{-5}$ Pa s <sup>-1</sup> )	$dP/dt$ (PhSPA) <sup>g</sup> ( $10^{-5}$ Pa s <sup>-1</sup> )	PhSPA <sup>h</sup> effect
BeO	10.6	15				0	0	no
MgO	8.7	32.6	53	30	0.1626	0	0	no
Al <sub>2</sub> O <sub>3</sub>	9.5	4.2	8.0	8.0	0.1905	0	0	no
MgAl <sub>2</sub> O <sub>4</sub>	8	12				0	0	no
SiO <sub>2</sub>	10	0.30	1.0	1.0	0.3333	0	0	no
TiO <sub>2</sub>	3.2	8.6	-9.0	-23	-0.1047	2.0	2.0	no
GeO <sub>2</sub>		8.5	2.0	2.0	0.0235	3.0	3.0	no
SnO <sub>2</sub>	3.8	10.2	-5.0	2.0	-0.0490	101	92	no
ZnO	3.2	4.4	-8.0	-19	-0.1818	120	37	negative
Sc <sub>2</sub> O <sub>3</sub>	6.0	40.2	88	88	0.2189	0	0	no
Y <sub>2</sub> O <sub>3</sub>	6.2	24.2	34	22	0.1405	8.0	8.0	no
La <sub>2</sub> O <sub>3</sub>	5.4	9.9	45	34	0.4546	81	155	yes
Sm <sub>2</sub> O <sub>3</sub>	5	15.2	40	41	0.2631	90	150	yes
Gd <sub>2</sub> O <sub>3</sub>	5.3	18	25		0.1389	3.0	62	yes
Dy <sub>2</sub> O <sub>3</sub>	5	90				84	81	no
Yb <sub>2</sub> O <sub>3</sub>	5.2	36	80	75	0.2222	2.8	30	yes
ZrO <sub>2</sub>	5.0	68.9	106	149	0.1539	12	320	yes
Y*ZrO <sub>2</sub> (5.5%)		71	50	60	0.0704	2.0	138	yes
Y*ZrO <sub>2</sub> (8%)		37	80	90	0.2162	1.0	93	yes
Y*ZrO <sub>2</sub> (15%)		30	110	120	0.3667	1.0	49	yes
HfO <sub>2</sub>	5.5	58.1	173	174	0.2978	8.0	83	yes

<sup>a</sup> Band-gap energy of the insulator or semiconductor specimen. <sup>b</sup> Extent of coloration of the specimen in vacuo. <sup>c</sup> Extent of photobleaching of a colored specimen in vacuo. <sup>d</sup> Extent of photobleaching in the presence of oxygen. <sup>e</sup> Fraction of photobleached color centers after 200 s of visible irradiation. <sup>f</sup> Rate of photoadsorption of oxygen. <sup>g</sup> Rate of photostimulated post-adsorption of oxygen. <sup>h</sup> Presence or absence of a photostimulated post-adsorption effect in the case of oxygen.

The principal objectives of this study were 2-fold. First, we wished to establish whether spectral sensitization of metal oxides by UV pre-illumination is a more general phenomenon than otherwise imagined, and whether it can be extended to photostimulated adsorption of molecules and to photochemical reactions. Second, we wished to confirm whether excitation of metal oxides in the absorption bands of photoinduced color centers is responsible for the red shifts of the spectral limits of photoreactions as evidenced in the case of alkali metal halides. In the present study we tested 21 metal oxides to ascertain the effect of photoinduced spectral sensitization. Zirconia, scandia, and spinel specimens were examined in some detail.

### Experimental Section

The 21 powdered metal oxide samples (Table 1) examined in preliminary tests were of "high purity grade". Three of these were studied in some detail. The powdered monoclinic form of ZrO<sub>2</sub> (IREA) was produced from zirconium chloroxide; specific surface area (BET with nitrogen gas) of the sample was  $\sim 7$  m<sup>2</sup> g<sup>-1</sup>. Powdered Sc<sub>2</sub>O<sub>3</sub> (IREA) and optical material grade spinel MgAl<sub>2</sub>O<sub>4</sub> were obtained from the Vavilov State Optics Institute; BET specific surface areas are  $\sim 9$  m<sup>2</sup> g<sup>-1</sup> and  $\sim 14$  m<sup>2</sup> g<sup>-1</sup>, respectively. Average crystal size was ca. 1  $\mu$ m. These three specific metal oxides were analyzed for content of impurities in their preparations: analyses for ZrO<sub>2</sub> gave  $6 \times 10^{-5}\%$  Fe, and less than  $5 \times 10^{-5}\%$  for Mn, Cu, Co, Cr, and Ti; for Sc<sub>2</sub>O<sub>3</sub>, analyses gave  $1 \times 10^{-5}\%$  Cu,  $2 \times 10^{-5}\%$  for Cr, Mn, and Ni,  $1 \times 10^{-4}\%$  Yb,  $2 \times 10^{-4}\%$  for V, Er, and Nd,  $3 \times 10^{-4}\%$  Fe, and  $1 \times 10^{-3}\%$  Y; for MgAl<sub>2</sub>O<sub>4</sub>, analyses gave  $5 \times 10^{-4}\%$  Cr,  $3 \times 10^{-3}\%$  Mn, and  $5 \times 10^{-3}\%$  Ca and Fe.

Any adventitious organic impurity and molecules adsorbed on the surface of the metal oxide specimens were removed by thermal pretreatment ( $T = 800$  K) first in an O<sub>2</sub> atmosphere ( $P = 100$  Pa) and then in vacuo. Reproduction of the original state of the samples between experiments was achieved by heating the samples in oxygen for ca. 1 h. Any experimental error in the spectral measurements caused by the nonreproducibility of the original state of the sample does not exceed about 5%.

**Metal Oxide Samples.** Zirconia (ZrO<sub>2</sub>;  $E_{bg} \approx 5.0$  eV) is a photoadsorbent and an active photocatalyst in accordance with empirical correlations between the photochemical activity of the metal oxide specimen and its band-gap energy  $E_{bg}$ .<sup>4</sup> The red limit of the photostimulated adsorption of O<sub>2</sub>, H<sub>2</sub>, CH<sub>4</sub>, and C<sub>2</sub>H<sub>6</sub> molecules on powdered ZrO<sub>2</sub><sup>12,13</sup> is positioned in the *extrinsic* absorption band region at about 3.0 eV ( $\lambda = 410$  nm). The first stage of photooxidation of methane and ethane is photostimulated adsorption followed by conversion to other hydrocarbons.<sup>12</sup> The quantum yield  $\Phi$  of photooxidation of propene over powdered zirconia is ca. 0.03;<sup>16</sup>  $\Phi$  of photostimulated adsorption of O<sub>2</sub> reaches 0.05 on irradiation of ZrO<sub>2</sub> at the red edge of the fundamental absorption band.<sup>17</sup> The main types of preexisting *intrinsic* defects in ZrO<sub>2</sub> are anion vacancies, V<sub>a</sub>.<sup>18</sup> Zirconia powder is photocolored under UV-excitation owing to formation of stable defects (color centers) with trapped electrons (Zr<sup>3+</sup>, F<sup>+</sup>, F)<sup>12,19</sup> or with trapped holes (O<sup>-</sup>-like V centers).<sup>12,20</sup> Color centers localized at the surface serve as long-lived adsorption centers (i.e., post-adsorption centers) for acceptor (e.g., O<sub>2</sub>) and donor (e.g., H<sub>2</sub> and CH<sub>4</sub>) molecules, respectively.<sup>21</sup>

Scandium oxide (Sc<sub>2</sub>O<sub>3</sub>) is a wide band gap insulator ( $E_{bg} = 6.0$  eV) with a cubic crystal lattice belonging to the T<sub>h</sub><sup>7</sup> space group; lattice constant,  $a = 9.845$  Å. Among the wide band gap metal oxides, Sc<sub>2</sub>O<sub>3</sub> is not as frequently used in photocatalytic studies as zirconia. Nonetheless, it is an active metal oxide in water photolysis in a gas/solid system.<sup>22</sup> Photoadsorption of O<sub>2</sub>, H<sub>2</sub>, and CH<sub>4</sub>, and methane photooxidation to CO<sub>2</sub> and H<sub>2</sub>O, along with its conversion to ethane, ethylene, and other hydrocarbons have also been established.<sup>14,23</sup> Photo- and radiation-induced color centers of the F- and V-type display complex spectra in the near-UV and visible spectral regions.<sup>14,24,25</sup>

Spinel, MgAl<sub>2</sub>O<sub>4</sub>, is a complex wide band gap ( $E_{bg} = 7.5 - 9.0$  eV<sup>26,27</sup>) insulator with a cubic crystal lattice and spinel-type structure F<sub>d3m</sub>; lattice constant,  $a = 8.11$  Å. Cation vacancies, V<sub>c</sub>, are the predominant type of *intrinsic* defects. In addition, synthetic spinels are partly ( $\leq ca.$  20%) inverted, whereby a fraction of the Mg<sup>2+</sup> cations occupy the positions of

$\text{Al}^{3+}$  ions and in turn the  $\text{Mg}^{2+}$  positions are occupied by  $\text{Al}^{3+}$  cations.<sup>28</sup> Such defects serve as hole and electron traps, respectively. Among the several UV- and radiation-induced centers, F and V centers have been identified in  $\text{MgAl}_2\text{O}_4$ .<sup>28–30</sup> Photoadsorption of  $\text{O}_2$ ,  $\text{H}_2$ , and  $\text{CH}_4$  and its influence on the photocoloration of spinel  $\text{MgAl}_2\text{O}_4$  have also been explored.<sup>29,31</sup>

**Procedures.** Powdered specimens were contained in a quartz cell (path length, 3 mm; illuminated area, 7 cm<sup>2</sup>) connected to a high-vacuum setup equipped with an oil-free pumping system; the ultimate gas pressure in the reaction cell was ca.  $10^{-7}$  Pa. The volume of the reactor occupied by the gas was 40 cm<sup>3</sup>. A Pirani-type manometer (sensitivity, 18 mV Pa<sup>-1</sup> for  $\text{O}_2$  and 24 mV Pa<sup>-1</sup> for  $\text{H}_2$ ) was used to measure gas pressures in kinetic studies. Analyses of gas composition were carried out using a mass spectrometer model MX-7301. Irradiation of the solid samples was accomplished with a 120 W high-pressure mercury lamp model DRK-120 (MELZ). Cutoff filters from a standard set of colored glass filters (Vavilov SOI) were used to select the spectral regions for sample excitation.

Diffuse reflectance spectra (vs  $\text{BaSO}_4$ ) were recorded with a Specord M-40 (Karl Zeiss, Jena, Germany) spectrophotometer equipped with an integrating sphere assembly; data processing was carried out using the Data Handling I package. In preliminary test experiments, a specially designed integrating sphere interfaced to a computer was employed; it permitted measurements of diffuse reflectance coefficients integrated in the visible spectral range between 400 and 800 nm (powdered samples); accuracy of the measurements,  $\pm 0.0001$ . Unless noted otherwise, the moveable high-vacuum setup/quartz cell system was moved as a unit between the position of irradiation and thermal treatment of the sample to a position for recording spectra; both were fixed with high precision in appropriate positions. Thermostimulated luminescence was recorded with a KSVU-12 (LOMO) spectral setup adapted to record emission from solid powders in vacuo and in a gaseous atmosphere. The heating rate of the specimens in the linear heating regime was maintained at 0.3 K s<sup>-1</sup>.

**Test Experiments.** Preliminary studies were conducted on 21 wide band gap metal oxides (Table 1) to diagnose the effect of photoinduced spectral sensitization for a simple surface photochemical process, namely photostimulated adsorption of oxygen. This set of experiments was carried out using the following uniform procedure:

(1) The integrated diffuse reflectance coefficient  $R_0$  was measured for each metal oxide specimen after sample pretreatment (see above).

(2) Samples were irradiated in vacuo for ca. 200 s using all the wavelengths of light from the mercury lamp, followed by a 10-min pause to permit the phosphorescence emission (typical of some oxides) to decay completely. The integrated diffuse reflectance coefficient  $R_{\text{hv}}$  was also measured to determine  $\Delta R = \{R_{\text{hv}} - R_0\}$  so as to characterize the extent of photocoloration (column  $\Delta R_{\text{vac}}$ ; Table 1).

(3) After addition of oxygen into the reactor ( $P_{\text{O}_2} = 1.5$  Pa), the system was exposed to the dark for about 10 min until post-adsorption of oxygen (also typical of some metal oxides) was complete. Subsequently, a given system was irradiated in the visible region using a 400-nm cutoff filter and the kinetics of photostimulated adsorption of oxygen determined (see Figure 1).

(4) A set of control experiments were also carried out for nonirradiated samples to establish the existence and the extent of photoadsorption of oxygen on a given metal oxide stimulated by visible light ( $\lambda \geq 400$  nm).

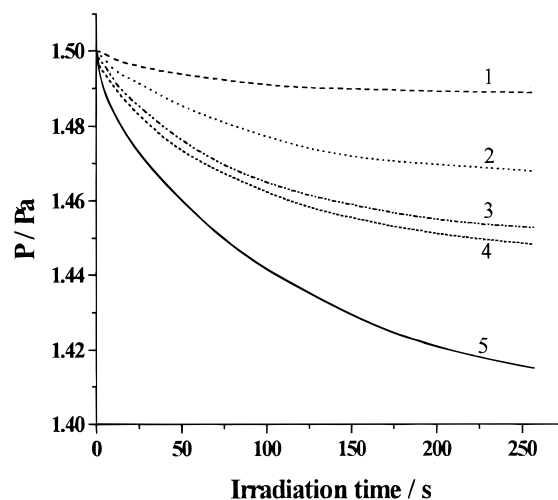


**Figure 1.** Kinetic curves as  $P$  versus time for the photostimulated post-adsorption of  $\text{O}_2$  on: (1)  $\text{Yb}_2\text{O}_3$ ; (2)  $\text{Gd}_2\text{O}_3$ ; (3)  $\text{HfO}_2$ ; (4)  $\text{Sm}_2\text{O}_3$ ; and (5) Y-stabilized  $\text{ZrO}_2$ .

(5) The effect of photostimulated post-adsorption of oxygen was considered established for irradiated samples when oxygen pressure changes under irradiation with visible light ( $\lambda > 400$  nm for ca. 600 s) exceeded 0.01 Pa and the rate of photoadsorption of oxygen was at least 10% higher than for non pre-irradiated samples. The extent of photobleaching of the UV-induced color  $\delta R_{\text{vac}} (= R_{\text{vis}} - R_{\text{hv}})$  and  $\delta R_{\text{O}_2} (= R_{\text{vis}} - R_{\text{hv}})$  was also measured;  $R_{\text{vis}}$  is the integrated diffuse reflectance coefficient after irradiation with visible light in vacuo and in oxygen, respectively (Table 1).

## Results

UV pre-irradiation of the samples decreases the integrated diffuse reflectance coefficients  $R_0$  ( $\Delta R$  varies from 0.0003 for  $\text{SiO}_2$  to 0.071 for the 5.5%Y-doped  $\text{ZrO}_2$  specimen) as evidenced by formation of photoinduced color centers for most of the metal oxides examined (Table 1). Detailed data concerning the changes in the diffuse reflectance characteristics and the influence of photoadsorption of gases on these features were reported earlier by Ryabchuck and Burukina.<sup>12</sup> Photobleaching of UV-induced color centers by visible light is typical for most of the metal oxides examined; relative values of  $\delta R_{\text{vac}}/\Delta R$  ratios range from 0.02 for  $\text{GeO}_2$  to 0.45 for  $\text{La}_2\text{O}_3$ . However, visible light irradiation decreases the integrated diffuse reflectance for  $\text{TiO}_2$ ,  $\text{SnO}_2$ , and for  $\text{ZnO}$  ( $\delta R_{\text{vac}} < 0$ ). The effect of photostimulated post-adsorption (PhSPA) was observed for  $\text{La}_2\text{O}_3$ ,  $\text{Sm}_2\text{O}_3$ ,  $\text{Yb}_2\text{O}_3$ ,  $\text{Cd}_2\text{O}_3$ ,  $\text{HfO}_2$ ,  $\text{ZrO}_2$ , and for  $\text{ZrO}_2$  stabilized in the cubic modification with  $\text{Y}_2\text{O}_3$ . Photostimulated adsorption (PhA) of  $\text{O}_2$  by visible light was not observed for  $\text{MgO}$ ,  $\text{BeO}$ ,  $\text{Sc}_2\text{O}_3$ ,  $\text{Y}_2\text{O}_3$ ,  $\text{SiO}_2$ ,  $\text{GeO}_2$ ,  $\gamma\text{-Al}_2\text{O}_3$ , and  $\text{MgAl}_2\text{O}_4$ , neither before nor after UV pre-irradiation of the specimens in vacuo. No difference in rates of  $\text{O}_2$  photoadsorption was detected between nonirradiated and UV-irradiated samples of  $\text{TiO}_2$ , whereas UV irradiation of  $\text{ZnO}$  caused a negative effect, i.e., decreased the rate of photoadsorption under visible light irradiation.

Thermostimulated adsorption of  $\text{O}_2$  takes place on UV-colored  $\text{ZrO}_2$ ,  $\text{Sm}_2\text{O}_3$ , and  $\text{Yb}_2\text{O}_3$ , but was not detected on nonpreirradiated samples. Maximal rates of thermostimulated  $\text{O}_2$  adsorption in the linear heating regime of the samples (see Experimental Section) were obtained at 420, 600, and 630 K for  $\text{ZrO}_2$ ,  $\text{Sm}_2\text{O}_3$ , and  $\text{Yb}_2\text{O}_3$ , respectively.

Photostimulated post-adsorption of  $\text{O}_2$  was not found for a group of metal oxides (from  $\text{BeO}$  to  $\text{SiO}_2$ , upper part in Table

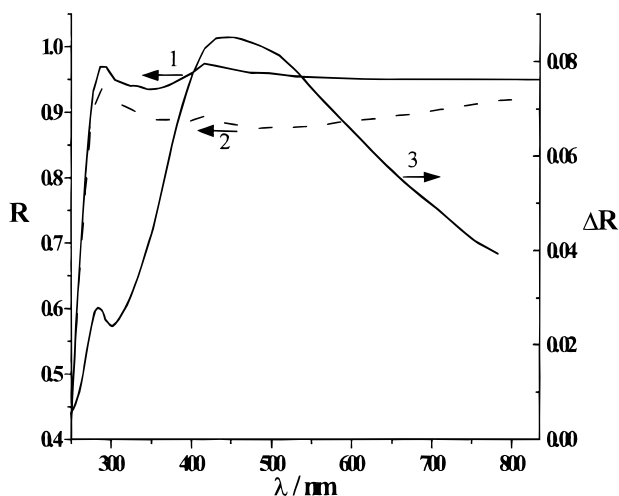


**Figure 2.** Diffuse reflectance spectra of powdered  $\text{ZrO}_2$ : (1) nonirradiated  $R_0$ ; (2) irradiated in vacuo  $R_{nv}$ ; (3) absorption spectrum given as  $\Delta R = R_0 - R_{nv}$  of photoinduced color centers.

1) whose band-gap energies  $E_{bg}$  are greater than 8 eV. Except for  $\text{MgO}$ , all these specimens are poorly photocolored ( $\Delta R < 0.015$ ) by the UV light used ( $\lambda \geq 200$  nm;  $E_{hv} \leq 6.2$  eV). Only *intrinsic* and *extrinsic* defects are photoexcited in these oxides. On the other hand, the metal oxides from  $\text{TiO}_2$  to  $\text{ZnO}$  with  $E_{bg}$  around 3 eV also displayed no photostimulated post-adsorption of  $\text{O}_2$ . The remaining oxides from  $\text{Sc}_2\text{O}_3$  to the Y-stabilized  $\text{ZrO}_2$  have  $E_{bg}$  around 5 eV; they show moderate to strong coloration ( $\Delta R > 0.02$ ) and photobleaching effects ( $\delta R_{vac}/\Delta R > 0.15$ ). Oxygen has an influence on the photobleaching of these oxides (positive: increase of photobleaching  $\delta R_{vac} < \delta R_{O_2}$ ; negative:  $\delta R_{vac} > \delta R_{O_2}$ ). However, there seem to be no correlations between the rates of photostimulated post-adsorption  $\{dP/dt (\text{PhSPA})\}$  and the remaining parameters (e.g.,  $\Delta R$ ) listed in Table 1.

Clearly, results from the preliminary studies show that UV-induced photocoloration of metal oxides is a necessary but not a sufficient condition to observe either photostimulated or thermostimulated post-adsorption of  $\text{O}_2$  on the metal oxide surfaces. Except for  $\text{ZnO}$ , all the metal oxides tested can be classed into two groups as regards the effect of photostimulated post-adsorption of  $\text{O}_2$ . Note that the thermostimulated post-adsorption effect for  $\text{O}_2$  was also detected for metal oxides which are otherwise also active in the photostimulated post-adsorption process.

To better understand the mechanism and the reasons underlying the photo- and thermo-stimulated processes on the surface of UV-colored metal oxides, we selected  $\text{ZrO}_2$  (strong effect of photostimulated post-adsorption of  $\text{O}_2$ ) from the first group and  $\text{Sc}_2\text{O}_3$  and  $\text{MgAl}_2\text{O}_4$  (no effect found) from the second group of metal oxides for a more detailed exploration of these processes.

**Zirconia,  $\text{ZrO}_2$ .** The spectral limit of surface photochemical processes of photoadsorption of  $\text{H}_2$ ,  $\text{CH}_4$ , and  $\text{O}_2$ , as well as the photoinduced coloration (formation of defects) of  $\text{ZrO}_2$  is positioned at about 410 nm. UV irradiation of powdered  $\text{ZrO}_2$  in vacuo with light of wavelength  $\lambda < 410$  nm caused the appearance of an additional broad absorption band (Figure 2). As evidenced from the results of previous studies,<sup>13,19,20</sup> this band is formed by an overlap of absorption bands of electron color centers F,  $\text{F}^+$ , and  $\text{Zr}^{3+}$  with maxima at 620, 390, and 280 nm, respectively, and of hole color centers of the V-type showing maxima at ca. 410 and 270 nm. When photoinduced

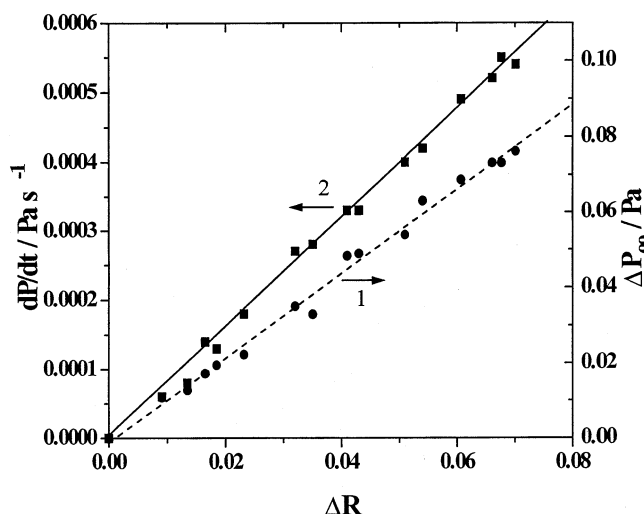


**Figure 3.** Dependencies of (1) the kinetic parameter  $\Delta P_\infty$ , and of (2) the initial rate of photostimulated post-adsorption of  $\text{O}_2$  on  $\text{ZrO}_2$  on the extent of photoinduced coloration  $\Delta R$ .

color centers are formed in the bulk of  $\text{ZrO}_2$  by UV pre-irradiation of the sample, the spectral limits of photostimulated adsorption are red-shifted to 580 nm for  $\text{H}_2$  and  $\text{CH}_4$  and to wavelengths above 800 nm for  $\text{O}_2$ ; these correspond to the positions of the absorption bands of V- and F-type color centers, respectively. Photostimulated adsorption of  $\text{CH}_4$  followed by secondary chemical reactions leads to formation of higher hydrocarbons:  $\text{C}_2\text{H}_6$ ,  $\text{C}_2\text{H}_4$ ,  $\text{C}_3\text{H}_8$ , along with  $\text{CO}_2$  and  $\text{H}_2\text{O}$ . The mass spectral analyses of the gas phase during the photostimulated post-adsorption of  $\text{CH}_4$ , and the temperature desorption spectra recorded after irradiation of  $\text{ZrO}_2$ , demonstrate the evolution of  $\text{C}_2\text{H}_6$  into the gas phase and formation of  $\text{C}_2\text{H}_6$ ,  $\text{C}_2\text{H}_4$ , and other reaction products on the specimen's surface. Identical reaction products were reported earlier when photoadsorption of  $\text{CH}_4$  on  $\text{ZrO}_2$  and other wide band gap metal oxides was examined under UV-light irradiation.<sup>23</sup>

The kinetics of photostimulated photoadsorption of  $\text{O}_2$  and  $\text{H}_2$  on  $\text{ZrO}_2$  follow the Solonitsyn approximation (eq 1):

$$\Delta P(t) = \Delta P_\infty \left\{ \frac{t}{t + \tau} \right\} = \Delta P_\infty \left\{ \frac{k\rho t}{k\rho t + 1} \right\} \quad (1)$$

where  $\Delta P(t)$  describes the temporal change in gas pressure (corresponds to the amount of photoadsorbed gas molecules) during irradiation for a time  $t$ ,  $\Delta P_\infty$  denotes the maximal coverage of photoadsorbed molecules on the surface at some given conditions when the time of irradiation approaches infinity ( $t \rightarrow \infty$ ), and  $\tau$  is the time of half-decay of the pressure during the photoprocess;  $\tau = (k\rho)^{-1}$ , and  $\rho$  is the photon flow (photons  $\text{cm}^{-2} \text{s}^{-1}$ ). The initial rate of photoadsorption is described by eq 2:

$$\left\{ \frac{dP}{dt} \right\}_{t \rightarrow 0} = \frac{\Delta P_\infty}{\tau} = \Delta P_\infty k\rho \quad (2)$$

Note that the linear dependence of the initial rates of photostimulated post-adsorption on light intensity (photon flow) was experimentally confirmed in special tests for all the metal oxides examined. The dependencies of  $\Delta P_\infty$  and the initial rate of photoadsorption  $\{dP/dt (\text{PhA})\}$  of  $\text{O}_2$  on powdered  $\text{ZrO}_2$  on the number of photoinduced color centers, represented by  $\Delta R$ , under photoexcitation with 436-nm light are illustrated in Figure 3. The linear dependence of the initial rate on the absorbance of the color centers  $\Delta R$  infers that the quantum yield

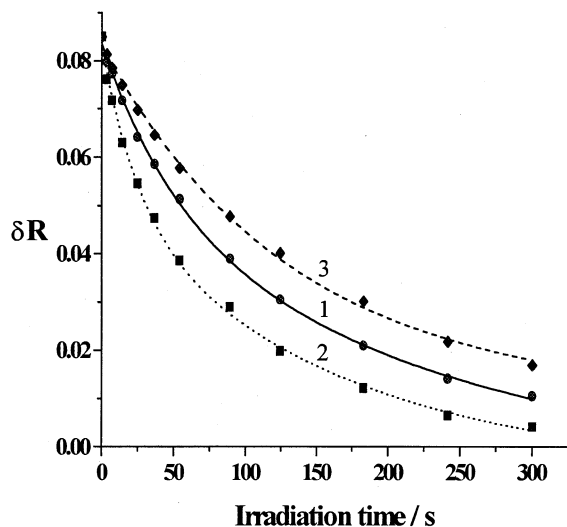


**Figure 4.** Kinetic dependencies of the photobleaching of color centers in  $\text{ZrO}_2$  by the actinic light at 436 nm (1) in vacuo, (2) in  $\text{O}_2$ , and (3) in  $\text{H}_2$ .

of photoadsorption of  $\text{O}_2$  ( $\Phi_{\text{O}_2}$ ) is independent of  $\Delta R$  for the whole range of coloration. Herein, we define<sup>14,24</sup> the quantum yield of photostimulated post-adsorption in relation to the rate by which photons are absorbed by the UV-induced color centers as

$$\Phi_{\text{O}_2} = \frac{dN/dt}{\Delta R \rho} \quad (3)$$

where the rate  $dN/dt \sim dP/dt$  is expressed by the number of adsorbed molecules per second. Under our experimental conditions, the quantum yield of photostimulated post-adsorption of  $\text{O}_2$  at  $\lambda = 436$  nm is  $\Phi_{\text{O}_2} = 0.16 \pm 0.02$ , whereas the corresponding quantum yield for  $\text{H}_2$  at this wavelength is  $\Phi_{\text{H}_2} = 0.057 \pm 0.007$ .

Irradiation of UV-colored  $\text{ZrO}_2$  in vacuo or in a gaseous atmosphere with visible light causes photobleaching of the color centers that is typical of many other metal oxides (see above). The relevant kinetics in vacuo in  $\text{O}_2$  and in  $\text{H}_2$  are displayed in Figure 4. The presence of  $\text{O}_2$  increases the rate of photobleaching of electron color centers in  $\text{ZrO}_2$ , whereas the presence of  $\text{H}_2$  decreases the rate. Using the data for the calibration of the absorbance  $\Delta R$  of F-type color centers in  $\text{ZrO}_2$  reported by Burukina and co-workers,<sup>17</sup> we estimate the quantum yield of photobleaching of F centers in vacuo,  $\Phi_{\text{F(vac)}}$ , relative to the number of photons absorbed by the color centers (see above) to be  $\Phi_{\text{F(vac)}} = 0.32 \pm 0.03$  at 436 nm, whereas in the presence of  $\text{O}_2$  and in the presence of  $\text{H}_2$  they are  $\Phi_{\text{F(O}_2)}} = 0.52 \pm 0.04$  and  $\Phi_{\text{F(H}_2)}} = 0.22 \pm 0.04$ , respectively.

The linear heating regime of a UV-colored  $\text{ZrO}_2$  powdered specimen in the presence of  $\text{O}_2$  leads to thermostimulated adsorption of  $\text{O}_2$  with a maximum rate obtained at 420 K, which also corresponds to the thermostimulated green luminescence (TSL) maximum of  $\text{ZrO}_2$ . The estimated activation energy of this TSL is  $E_a = 1.1 \pm 0.1$  eV. No thermostimulated adsorption was detected on noncolored samples.

**Scandium Oxide,  $\text{Sc}_2\text{O}_3$ .** Scandium oxide is representative of the second group of metal oxides which displayed no spectral sensitization for the photoadsorption of  $\text{O}_2$  (see above). Results of detailed studies on the interconnection between photoinduced formation and destruction of defects with surface photochemical processes on  $\text{Sc}_2\text{O}_3$  specimens have been reported elsewhere.<sup>14,24</sup>

The spectral limit of photoinduced defect formation in the bulk and photostimulated adsorption of  $\text{O}_2$ ,  $\text{H}_2$ , and  $\text{CH}_4$  on the

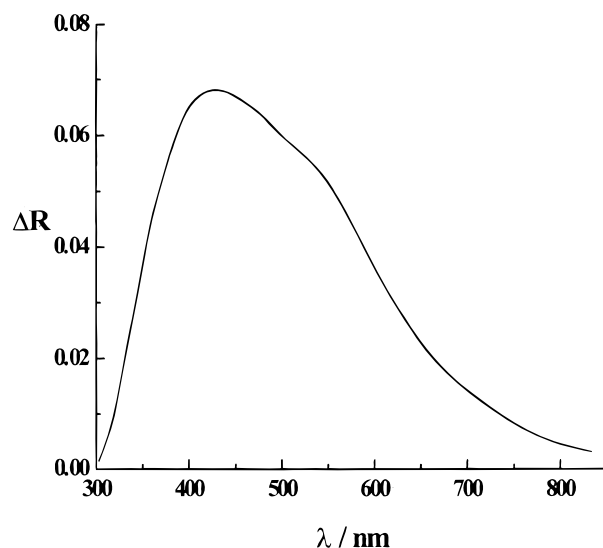


**Figure 5.** Absorption spectrum  $\Delta R$  of photoinduced color centers in powdered  $\text{Sc}_2\text{O}_3$ .

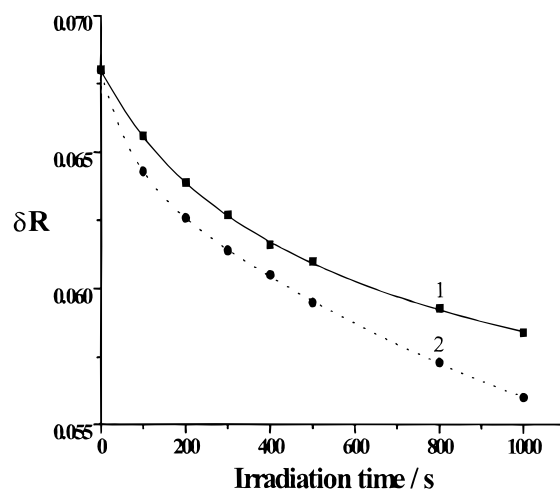


**Figure 6.** Kinetic dependencies of the photobleaching of color centers in  $\text{Sc}_2\text{O}_3$  by the actinic light at 436 nm (1) in vacuo and (2) in  $\text{H}_2$ .

surface of powdered  $\text{Sc}_2\text{O}_3$  is located at ca. 320 nm. UV-irradiated powdered scandia shows a broad absorption band at  $\lambda_{\text{max}} 430$  nm which consists of overlapping bands of hole color centers and (probably also) electron F-type color centers with  $\lambda_{\text{max}}$  at 330 nm (Figure 5). The spectral limits of photostimulated interaction of gases with the surface of the preirradiated sample is red-shifted to 360 nm for  $\text{O}_2$  and to 560 nm for  $\text{H}_2$  and  $\text{CH}_4$ . The kinetics of photostimulated post-adsorption of  $\text{H}_2$  and  $\text{O}_2$  on excitation of the photoinduced color centers are described by eq 1. The parameter  $\Delta P_\infty$  scales linearly with the extent of coloration  $\Delta R$ , whereas the dependence of the initial rate of photoadsorption of  $\text{H}_2$  on  $\Delta R$  tends to be sublinear, indicating that the quantum yield of photostimulated adsorption of  $\text{H}_2$  decreases with increasing  $\Delta R$ .<sup>14</sup>

Irradiation of UV-colored  $\text{Sc}_2\text{O}_3$  with visible light leads to photobleaching of the color centers, the rate of which increases in the presence of  $\text{H}_2$  and does not change in the presence of  $\text{O}_2$  relative to the rate of the photoprocess in vacuo (see Figure 6). The linear dependence between the concentration of adsorbed  $\text{H}_2$  and the difference between the number of color centers photobleached in  $\text{H}_2$  and in vacuo has been confirmed (see Figure 7). Heating the UV-colored powdered scandia in the linear regime causes adsorption of  $\text{H}_2$  which correlates with the

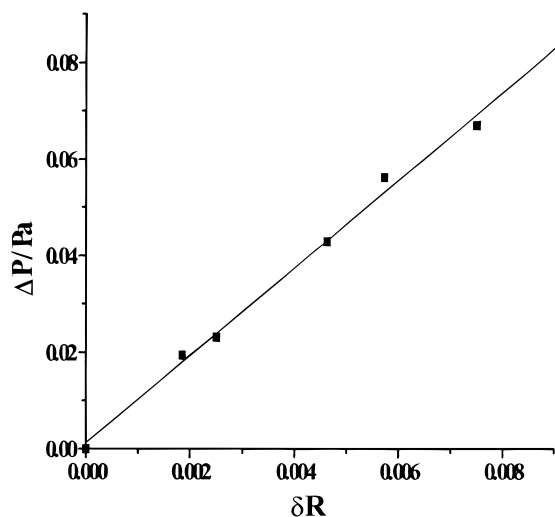


**Figure 7.** Dependence of the amount of adsorbed  $H_2$ ,  $\Delta P$ , during the photostimulated post-adsorption on the number of bleached color centers  $\delta R$ .

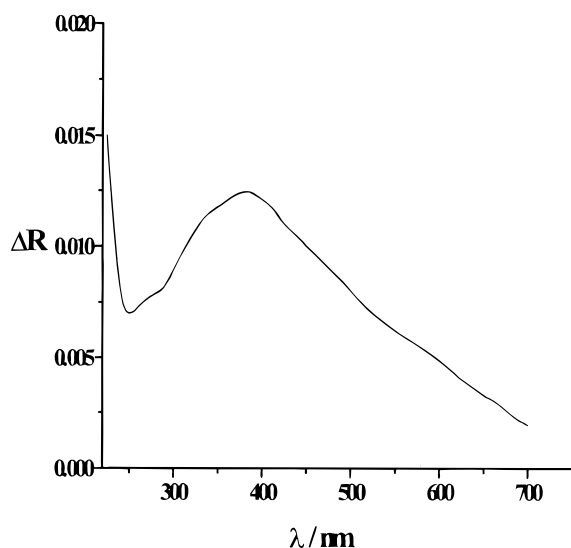


**Figure 8.** Absorption spectrum  $\Delta R$  of photoinduced color centers in powdered  $MgAl_2O_4$ .

thermoannealing of hole color centers. No adsorption of  $H_2$  occurred on noncolored samples.<sup>14</sup>

Secondary reactions that follow the photostimulated adsorption of  $CH_4$  during photoexcitation of hole color centers with visible light convert  $CH_4$  to higher hydrocarbons such as  $C_2H_6$ ,  $C_2H_4$ , and  $C_3H_8$ , among others.

**Spinel,  $MgAl_2O_4$ .** Spinel belongs to the second group of metal oxides examined (Table 1). It displays no photochemical activity toward  $O_2$  when spinel is irradiated with visible light, neither before nor after UV pre-irradiation in vacuo. Nonetheless, spinel specimens are photoactive with respect to UV-stimulated adsorption of  $H_2$ ,  $O_2$ ,  $CH_4$ , and  $CO$ .<sup>31</sup> The spectral limit of these surface photochemical processes and photoinduced formation of defects occurs at ca. 260 nm when the specimen was not preirradiated. UV-irradiated powdered spinel (in vacuo) displays a broad absorption band at  $\lambda_{max} \sim 390$  nm, attributable to formation of different photoinduced hole color centers (Figure 8).<sup>28,30</sup> The spectral limit of photoadsorption of  $H_2$  and  $CH_4$  is red-shifted from 260 nm to ca. 410 nm after UV-induced coloration of the powdered spinel specimen. No red shift was detected for photoadsorption of  $O_2$  because absorption by electron color centers occurs at  $\lambda < 260$  nm. Pre UV irradiation

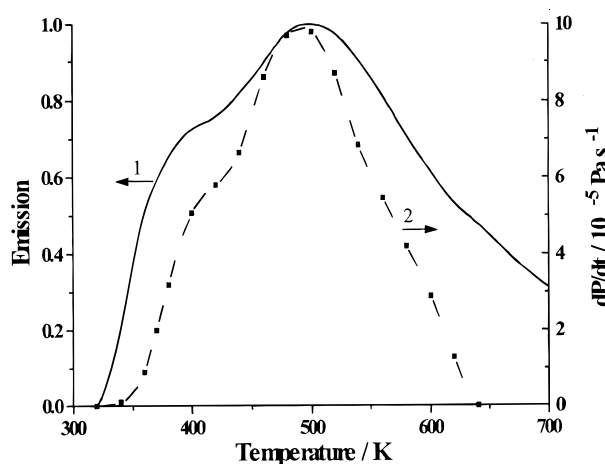


**Figure 9.** Temperature dependence of the (1) thermoluminescence and (2) thermostimulated post-adsorption of hydrogen on  $MgAl_2O_4$ .

of a spinel sample in vacuo increases the rate of photostimulated adsorption of  $O_2$  by up to ca. 20%. Irradiation of UV-colored samples with light in the range  $300 \text{ nm} < \lambda < 400 \text{ nm}$  affects photobleaching of hole color centers. A decrease in the coloration of spinel was also observed during thermal treatment of the colored sample in the linear heating regime. Concomitantly, the thermostimulated luminescence and the thermostimulated adsorption of  $H_2$  were detected for colored spinel (see Figure 9); both dependencies correlate with each other. Neither thermostimulated luminescence nor thermostimulated adsorption were observed for noncolored spinel specimens.

## Discussion

Most metal oxides belong to the class of photoresistant solids. The only mechanism of defect formation caused by light in such solids is photocarrier trapping by preexisting *intrinsic* and *extrinsic* lattice defects to yield so-called color centers. An example of this kind of defect formation is trapping of photogenerated electrons by anion vacancies to give F-type color centers. A thorough discussion of the mechanisms of processes which lead to formation of defects is given elsewhere.<sup>7,32-36</sup>

Photoinduced centers differ from each other by the energy distance,  $E_d$ , between the level of the trapped carrier within the energy band gap of the insulator or semiconductor and the bottom of the conduction band for electron centers, and the top of the valence band for hole centers.<sup>35,37,38</sup> From this point of view, a given photoinduced center can be described as a shallow center (or trap) if the energy of the trapped carrier is comparable to the energy of thermal excitation of the crystal lattice (i.e.,  $E_d \sim kT$ ), or as a deep energy center if  $E_d \gg kT$ . The difference between the various types of photoinduced centers is determined by the dominant decay path back to the initial state (without trapped carrier).

In general, any photoinduced center can lose a carrier as a result of (i) thermal ionization with a thermal quenching probability given by  $q_{th}$ ; (ii) recombination with a charge carrier of the opposite sign for which the recombination probability is  $q_{rec}$ ; (iii) photoionization caused by incident photons,  $q_{ph}$ ; and (iv) tunneling recombination of adjacent hole and electron centers. The role of the latter process in heterogeneous systems has been treated extensively elsewhere.<sup>39-41</sup>

For the simplest case of centers with one trapped carrier, the kinetics of formation of centers typically follow an exponential growth and approach the steady-state concentration of photo-

induced defects  $N_d$  given by<sup>36</sup>

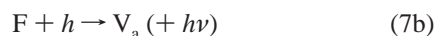
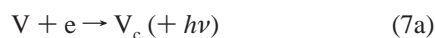
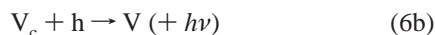
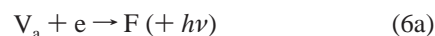
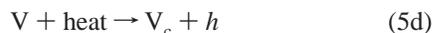
$$N_d = N_o \left\{ \frac{p}{p + q_{th} + q_{rec} + q_{ph}} \right\} \quad (4)$$

where  $N_o$  is the number of preexisting defects of a given type,  $p$  is the probability of photocarrier trapping defined, as are the corresponding quenching probabilities  $q$ , as the number of events per unit time. For shallow traps, the thermal ionization usually dominates, i.e.,  $q_{th} \gg q_{rec} + q_{ph}$ . By contrast, thermal ionization can be neglected for deep energy centers, i.e.,  $q_{th} \ll q_{rec} + q_{ph}$ . In the latter case, centers having a high ability to capture a carrier of the opposite sign,  $q_{rec} \gg p$ , can serve as effective recombination centers. These centers do not accumulate in considerable quantity in illuminated crystals since  $N_d = N_{rec} \ll N_o$  (eq 4). At the same time, recombination centers are mainly responsible for the steady-state concentrations of photogenerated carriers in wide band gap solids because of the inefficient direct band-to-band recombination compared with recombination involving deep energy centers.<sup>35</sup> Contrary to recombination centers, deep energy centers ( $q_{rec} \sim p$ ) accumulate in sufficient amount in solids under illumination. Such defects are the color centers because they usually have absorption bands located in the UV and visible regions and determine the lasting stable color of pre-illuminated, initially colorless wide band gap solids. Photoionization of color centers by the actinic light may, to some extent, reduce the color saturation level under illumination when  $q_{rec} \sim q_{ph}$ .

Results of test experiments demonstrate that the red shift of the spectral limits of photochemical processes on the surface of UV-preirradiated metal oxides may indeed be a general phenomenon. In fact, the photostimulated post-adsorption of  $O_2$  occurs for 9 of the 21 metal oxides tested. As evidenced by the results, the necessary condition to observe this effect is photoinduced formation of defects (color centers) during the preliminary UV irradiation of the samples. All the metal oxides investigated belong to the class of photoresistant solids, in which trapping of photocarriers by preexisting surface and bulk defects is the dominant mechanism of formation of color centers in these solids. Evidently, photobleaching of UV-induced color centers by visible light is identified with the effect of photostimulated post-adsorption of  $O_2$ . Notwithstanding that photobleaching is typical of all the metal oxides tested, the photostimulated post-adsorption event was detected only for 9 of the 21 samples. Moreover, ZnO displays a negative effect, i.e., the rate of the photoprocess decreases. To explain this observation, we note that up to 100% of the photoinduced electron active centers on the ZnO surface are stable at ambient temperatures with a lifetime as long as (at least) a few days.<sup>42</sup> We infer that during UV irradiation of ZnO in vacuo many of the surface active centers are created in a manner analogous to when  $O_2$  is present.

Exposing a UV-pre-irradiated sample of ZnO to  $O_2$  (in the dark) causes all the electron surface centers to be blocked by adsorbed  $O_2$  molecules, thereby inhibiting additional electron active centers from being created on the ZnO surface. This leads to a decrease in the rate of photostimulated adsorption of  $O_2$  by visible light after UV pre-irradiation.<sup>43</sup> However, the fraction of long-lived surface active centers does not exceed  $\sim 10\%$  for the majority of other metal oxides; UV pre-irradiation of these metal oxides in vacuo does not decrease the rate of surface photochemical processes. Reasons as to why photostimulated post-adsorption of  $O_2$  was not universally observed for the metal oxides of the second group necessitate certain considerations that emerge from detailed studies on the  $ZrO_2$ ,  $Sc_2O_3$ , and

$MgAl_2O_4$  specimens; the results suggest the following simplified mechanism:



where stages 5a, 5b and 5c, 5d represent the photo- and thermoionization (photobleaching and thermoannealing), respectively, of electron (F-type) and hole (V-type) color centers; stages 6a and 6b describe trapping of electrons and holes, respectively, by preexisting defects (e.g., anion  $V_a$  and cation  $V_c$  vacancies) to form electron (F) and hole (V) color centers; note that these processes may be accompanied by luminescence  $hv$ . Stages 7a and 7b represent the recombination of free electrons and holes, respectively, with trapped carriers of opposite sign localized at UV-induced defects that can also yield luminescence; however, recombination occurs primarily through recombination centers rather than through color centers (see above). Finally, stages 8a and 8b represent the first steps of surface photochemical reactions as a process of carrier trapping by either the surface defects to form surface active centers, or by the preadsorbed molecules to produce either anion radicals (electron trapping) or cation radicals (hole trapping), respectively. We denote all types of electron color centers in metal oxides (F,  $F^+$ , and  $Zr^{3+}$ ) as F-centers, whereas all the types of hole color centers ( $V$ ,  $V^-$ ,  $V^{2-}$ , and  $\{[Mg^{2+}]_{Al} O^-\}$ ) are described as V-centers.

Because of its acceptor character,  $O_2$  reacts predominantly with electrons to give such anion radicals as  $O_2^{\cdot-}$  and  $O^-$ ; the adsorption complex  $O_3^{\cdot-}$  formed by the interaction of  $O_2$  with a surface hole  $O_S^{\cdot-}$  is unstable at ambient temperatures on most metal oxides and has been detected only at low temperatures.<sup>23,42,44</sup> Thus to observe photostimulated adsorption of  $O_2$ , free electrons must be generated which can be achieved by visible light excitation of electron color centers. That is, UV-induced coloration in the visible spectral region must be due to electron color centers. This is the case for  $ZrO_2$  where UV irradiation causes the appearance of a broad absorption band in the visible region formed by an overlap of absorption bands of  $F^+$  and F centers (see Experimental Section). Excitation of these centers with visible light generates free electrons (stage 5a) which in turn produce electron active centers (stage 8a) that react with  $O_2$  molecules. On the basis of this mechanism and the steady-state approach for the concentration of carriers at sufficiently high  $O_2$  pressures (the case in our experiments), the expression for the initial rate of photoadsorption of  $O_2$  is given by<sup>45</sup>

$$\frac{d[S^-]}{dt} = \frac{k_{5a} k_{8a} [F] [S] \rho}{k_{6a} [V_a] + k_{7a} [V] + k_{8a} [S]} \quad (9)$$

where  $k_{5a}$ ,  $k_{6a}$ ,  $k_{7a}$ ,  $k_{8a}$  are the rate constants of the corresponding steps in the mechanism (5a–8b), and  $\rho$  is the photon flow of irradiation. It is worth noting that the initial concentration of F and V color centers and the concentration of anion vacancies,  $[V_a]$ , depend on the time of UV pre-irradiation and on the relationship (eq 10):

$$[V_a] = [V_{a0}] - [F] \quad (10)$$

where  $[V_{a0}]$  is the concentration before UV-induced coloration of the metal oxide specimen. Considering that  $[V] = (\text{const}) - [F]$  from the charge conservation law (see discussions in refs 27 and 28), and assuming that  $k_{6a} [V_{a0}] \gg \{k_{7a} (\text{const}) - k_{6a}\} - [F]$ , eq 9 reduces to

$$\frac{d[S^-]}{dt} = (\text{const}') [F] \rho \quad (11)$$

where  $k_{5a} k_{8a} / \{k_{6a} [V_a] + k_{8a} [S]\} = (\text{const}')$  such that the rate scales linearly with the absorption (i.e., concentration) of F color centers. (Note that  $[S]$  is constant since in the proposed mechanism it is assumed that pre-irradiation does not affect this concentration term).

To the extent that the rate of photon absorption is given by

$$\rho_{\text{abs}} = \sigma [F] \rho \quad (12)$$

where  $\sigma$  is the cross-section of photon absorption by F centers, the quantum yield of photoreaction will then be given by

$$\Phi = \frac{(\text{const}') [F] \rho}{\sigma [F] \rho} = (\text{const}'') \quad (13)$$

Thus,  $\Phi$  is independent of the concentration of color centers, and since  $\tau$  scales as  $\rho^{-1}$  (from eq 1), the kinetic parameter  $\Delta P_{\infty}$  is proportional to the concentration of F centers, i.e.,  $\Delta P_{\infty} \propto [F]$  (eqs 2 and 11). The experimental results obtained for  $\text{ZrO}_2$  are fully described by eqs 9, 11, and 13 (see Results and Figure 3).

The tail end of the complex absorption band of UV-induced hole color centers in  $\text{ZrO}_2$  occurs in the visible spectral region causing the spectral limit of the photostimulated adsorption of  $\text{H}_2$  to be red-shifted to ca. 580 nm. Irradiation of UV-colored  $\text{ZrO}_2$  by visible light at  $\lambda = 436$  nm leads to photoexcitation of electron and hole color centers (stages 5a and 5b). The rate of photobleaching of F centers can be written as:

$$\frac{d[F]}{dt} = -k_{5a} [F] \rho + k_{6a} [V_a] [e] - k_{7b} [F] [h] \quad (14)$$

with the steady-state concentrations of carriers given by

$$[e] = \frac{k_{5a} [F] \rho}{k_{6a} [V_a] + k_{7a} [V]} \quad \text{in vacuo} \quad (15a)$$

and

$$[h] = \frac{k_{5b} [F] \rho}{k_{6b} [V_c] + k_{7b} [F]} \quad \text{in vacuo} \quad (15b)$$

whereas in the presence of gases, they are given by

$$[e] = \frac{k_{5a} [F] \rho}{k_{6a} [V_a] + k_{7a} [V] + k_{8a} [S]} \quad \text{in oxygen} \quad (16)$$

and

$$[h] = \frac{k_{5b} [F] \rho}{k_{6b} [V_c] + k_{7b} [F] + k_{8b} [S]} \quad \text{in hydrogen} \quad (17)$$

We have neglected the concentrations of  $S^-$  and  $S^+$  centers in vacuo since their lifetime during irradiation with visible light does not exceed ca.  $10^{-2}$  s (i.e.,  $\tau \leq 10^{-2}$  s) and the fraction of these centers produced in vacuo does not exceed  $\sim 10\%$  of those created in the presence of either  $\text{O}_2$  or  $\text{H}_2$ .<sup>21</sup> Combination of eqs 14–17 yields:

$$\left(\frac{d[F]}{dt}\right)_{\text{vac}} - \left(\frac{d[F]}{dt}\right)_{\text{O}_2} = \frac{-d[S^-]}{dt} \quad (18)$$

$$\left(\frac{d[F]}{dt}\right)_{\text{vac}} - \left(\frac{d[F]}{dt}\right)_{\text{H}_2} = \frac{-d[S^+]}{dt} \quad (19)$$

so that

$$\Phi_{F(\text{O}_2)} - \Phi_{F(\text{vac})} = \Phi_{\text{O}_2} \quad (20)$$

and

$$\Phi_{F(\text{vac})} - \Phi_{F(\text{H}_2)} = 2 \Phi_{\text{H}_2} \quad (21)$$

which correspond to the experimental quantum yields of photobleaching of F centers in vacuo ( $\Phi_{F(\text{vac})} = 0.32 \pm 0.03$ ), in oxygen ( $\Phi_{F(\text{O}_2)} = 0.52 \pm 0.04$ ,  $\Phi_{\text{O}_2} = 0.16 \pm 0.02$ ), and in hydrogen ( $\Phi_{F(\text{H}_2)} = 0.22 \pm 0.03$ ,  $2\Phi_{\text{H}_2} = 0.11 \pm 0.02$ ) considering a dissociative adsorption for  $\text{H}_2$  on surface hole centers to give twice the value of the quantum yield of photogeneration of  $S^+$  surface active centers (eq 21).<sup>46</sup>

For  $\text{Sc}_2\text{O}_3$  and  $\text{MgAl}_2\text{O}_4$ , representatives of the second group of metal oxides, the UV-induced absorption in the visible spectral range is due to hole color centers.<sup>14,25,28,30</sup> Consequently, photoexcitation of these centers at  $\lambda > 400$  nm causes the photostimulated adsorption of donor molecules ( $\text{H}_2$  and  $\text{CH}_4$ ) and does not lead to adsorption of acceptor molecules (oxygen). We infer this to be the major cause for the lack of photostimulated adsorption of  $\text{O}_2$  on other metal oxides of the second group. Indeed, absorption bands in the visible spectral range for  $\text{MgO}$ ,<sup>47–49</sup>  $\text{Al}_2\text{O}_3$ ,<sup>50</sup>  $\text{BeO}$ ,<sup>47–49</sup>  $\text{Sc}_2\text{O}_3$ ,<sup>14,25</sup> and  $\text{MgAl}_2\text{O}_4$ <sup>28,30</sup> are those of hole color centers; absorption bands of electron color centers are seen in the UV spectral region. Consequently, electron color centers are not photoexcited under visible light irradiation conditions used herein (see Results), and photostimulated post-adsorption of donor molecules is to be expected for these metal oxides under photoexcitation with visible light. Photostimulated post-adsorption of acceptor molecules, e.g.  $\text{O}_2$ , is anticipated for these metal oxides when illuminated with UV light.

The red shift of the spectral limit to 360 nm observed for the photoadsorption of oxygen on  $\text{Sc}_2\text{O}_3$  corresponds to the absorption region of photoinduced F centers ( $\lambda_{\text{max}} \sim 350$  nm). In spinel, the absorption bands of UV-induced F color centers ( $\lambda_{\text{max}}$ , 240 and 260 nm) coincide with the spectral region of photoactive absorption of nonirradiated samples ( $\lambda \leq 260$  nm). There is no red-shift of the spectral limit of the photoactivity of this metal oxide within the experimental accuracy of our experiments, owing to the restriction imposed by the sharp cutoff of the optical filters used. However, photoinduced formation of electron color centers does lead to an increase in the rate of photoadsorption of  $\text{O}_2$ . Kuznetsov et al<sup>48</sup> have described a

similar behavior for the photoadsorption of O<sub>2</sub> on BeO, which they associated with a redistribution of carriers between preexisting F and F<sup>+</sup> centers under UV excitation.

Photoexcitation of hole color centers by visible light in Sc<sub>2</sub>O<sub>3</sub> and MgAl<sub>2</sub>O<sub>4</sub> (stage 5b) leads to photostimulated post-adsorption of donor molecules (H<sub>2</sub>, CH<sub>4</sub>, and CO) and to the photobleaching of coloration. By analogy with the effect of photostimulated post-adsorption of O<sub>2</sub> on ZrO<sub>2</sub> on the rate of photobleaching of F color centers (see above), we can write a similar expression to reflect the influence of photostimulated post-adsorption of donor molecules on the rate of photobleaching of hole color centers in Sc<sub>2</sub>O<sub>3</sub> and MgAl<sub>2</sub>O<sub>4</sub>; thus,

$$\left(\frac{d[V]}{dt}\right)_{\text{vac}} - \left(\frac{d[V]}{dt}\right)_{\text{H}_2} = \frac{d[S^+]}{dt} \quad (22)$$

or after integration

$$\Delta[V] = [S^+] \quad (23)$$

where  $\Delta[V]$  denotes the difference between the number of hole color centers destroyed in the presence of H<sub>2</sub> and in vacuo, and  $[S^+]$  is the number of adsorbed molecules or species.<sup>51</sup> Equations 22 and 23 are in accord with experimental results obtained in this study for Sc<sub>2</sub>O<sub>3</sub> (see Results and Figures 6 and 7). Taking into account that one molecule of H<sub>2</sub> occupies one surface hole center, S<sup>+</sup>, on the surface of scandia,<sup>14</sup> the experimental linear correlation between  $\delta R$  and  $\Delta P$  of H<sub>2</sub> (Figure 7) and with eq 23 we estimate the number of hole color centers (V) produced in our experiments by UV irradiation of Sc<sub>2</sub>O<sub>3</sub> to be  $[V] = (0.9 \times 10^{17})\Delta R = 6.1 \times 10^{15}$  centers after UV coloration ( $\Delta R$  was taken from Figure 5 at  $\lambda = 430$  nm).<sup>51</sup> If we further assume that during the UV irradiation only 5 to 10 layers of the microcrystals, average crystal size ca.  $10^{-4}$  cm, become colored because of strong *intrinsic* absorption, the concentration of V-type photoinduced color centers in Sc<sub>2</sub>O<sub>3</sub> are ca.  $(1-3) \times 10^{18}$  cm<sup>-3</sup> which is the typical defect concentration in commercial solid specimens. Knowledge of the number of hole color centers in colored Sc<sub>2</sub>O<sub>3</sub> now affords an estimate of the quantum yield of photobleaching of these centers:  $\Phi = 0.022 \pm 0.002$  in vacuo and  $0.046 \pm 0.003$  in a H<sub>2</sub> or CO atmosphere. The quantum yield of photostimulated adsorption of H<sub>2</sub> and CO on colored scandia is  $0.023 \pm 0.002$ ,<sup>14</sup> so that the quantum yield of photobleaching of hole color centers in H<sub>2</sub> (or CO) reflects the sum of the quantum yield of photobleaching of coloration in vacuo and the quantum yield of surface photochemical processes. It is noteworthy that two V-type color centers in Sc<sub>2</sub>O<sub>3</sub> are photobleached on adsorption of one H<sub>2</sub> molecule on the surface (ratio of quantum yields,  $0.046/0.023 = 2$ ; e.g., dissociation of H<sub>2</sub> into two hydrogen atoms to yield 2 H<sup>+</sup>), whereas the photostimulated post-adsorption of an acceptor O<sub>2</sub> molecule on the ZrO<sub>2</sub> surface implicates three F centers destroyed (quantum yield ratio,  $0.52/0.16 \approx 3$  for oxygen to yield three species, namely one O<sub>2</sub><sup>-•</sup> and two O<sup>-•</sup> ions).

Destruction of color centers can also be achieved by thermoionization (stages 5c and 5d) yielding free charge carriers. Trapping and recombination of these carriers is accompanied by (thermostimulated) luminescence (stages 6a, 6b, 7a, and 7b). At the same time, the carriers can migrate to the solid's surface and take part in surface chemical processes (stages 8a and 8b). Obviously, thermoannealing of hole color centers would lead to adsorption of donor molecules, whereas thermoionization of electron color centers would lead to surface reactions with acceptor molecules. Experimental correlation between the thermostimulated luminescence and the thermostimulated gas

adsorption observed for the ZrO<sub>2</sub>/O<sub>2</sub> and MgAl<sub>2</sub>O<sub>4</sub>/H<sub>2</sub> systems demonstrates the validity of the proposed mechanism described by stages 5a to 8b. In fact, it was established earlier<sup>52,53</sup> that the thermostimulated luminescence of ZrO<sub>2</sub> originates from the thermoionization of F-type color centers (stage 5c), that is, of anion vacancies with trapped electrons. In our experiments, this thermostimulated luminescence correlates with the adsorption of O<sub>2</sub>. In spinel, the thermostimulated luminescence emanates from ionization of V-type hole color centers (stage 5d) followed by retrapping or recombination of the free holes with the produced cation vacancies (stage 6b).<sup>54</sup> Appearance of free holes on the metal-oxide surface induces the thermostimulated post-adsorption of H<sub>2</sub> (Figure 9 and Results). Thermostimulated adsorption of H<sub>2</sub> on Sc<sub>2</sub>O<sub>3</sub> also results from the thermostimulated destruction of hole color centers.<sup>14</sup> By analogy, we infer that the thermostimulated adsorption of O<sub>2</sub> on the Sm<sub>2</sub>O<sub>3</sub> and Yb<sub>2</sub>O<sub>3</sub> surfaces (Table 1) is a result of the thermoannealing of electron color centers in these metal oxides.

### Concluding Remarks

The data reported here emphasize the notion that the influence of spectral sensitization on surface photochemical processes by preliminary UV irradiation of the metal oxide specimens is encountered not only for the photostimulated adsorption of molecules, but also, taking CH<sub>4</sub> as an example, in the multistep chemical reaction of CH<sub>4</sub> oxidation and its conversion to higher hydrocarbons. The results also illustrate the relevance of the present studies in solving the problem of spectral sensitization of wide band gap solids in heterogeneous photocatalytic applications.

**Acknowledgment.** We are grateful to the Natural Science and Engineering Research Council (N.S.E.R.C.) of Canada for support. A.V.E. thanks N.S.E.R.C. for a North Atlantic Treaty Organization Science Fellowship for 1997 and 1998. We also thank Dr. A. A. Basov, Dr. G. K. Kuzmin, and N. S. Andreev of the University of St. Petersburg for designing the setup used in the measurement of the total reflectance.

### References and Notes

- (1) *Photocatalysis. - Fundamentals and Applications*; Serpone, N.; Pelizzetti, E., Eds.; John Wiley & Sons: New York, 1989.
- (2) *Semiconductor Nanoclusters - Physical, Chemical, and Catalytic Aspects*, Vol. 103 (Studies in Surface Science and Catalysis); Kamat, P. V.; Meisel, D., Eds.; Elsevier: Amsterdam, 1997.
- (3) Miller, R. J. D.; McLendon, G. L.; Nozik, A. J.; Schmickler, W.; Willig, F. *Surface Electron Transfer Processes*; VCH Publishers: New York, 1995.
- (4) Kisel'ov, V. Th.; Krilov, B. O. *Electronic Phenomena in Adsorption and Catalysis at Semiconductors and Insulators*; Nauka: Moscow, Russia, 1979.
- (5) Baru, V. G.; Volkenstein, Th. *The Effect of Irradiation on Surface Properties of Semiconductors*; Nauka: Moscow, Russia, 1978.
- (6) Photocatalytic Transformation of Solar Energy. *Heterogeneous, Homogeneous and Organized Molecular Structures*; Zamaraev, K. I.; Parmon, V. N., Eds. Nauka: Novosibirsk, Russia, 1991.
- (7) Luschnik, Ch. B.; Luschnik, A. Ch. *Decay of Electronic Excitation with Formation of Defects in Solids*; Nauka: Novosibirsk, Russia, 1989.
- (8) Hersh, H. N. *Phys. Rev.* **1966**, *148*, 928.
- (9) Pooley, D. *Proc. Phys. Soc.* **1966**, *87*, 257.
- (10) Vitols, I. K. *Izv. Akad. Nauk. USSR, Ser. Fiz.* **1966**, *30*, 564.
- (11) Bradford, J. N.; Williams, R. T.; Faust, W. L. *Phys. Lett.* **1975**, *35*, 300.
- (12) Ryabchuk, V. K.; Burukina, G. V. *Fiz. Khim.* **1991**, *65*, 1621.
- (13) Emeline, A. V.; Kataeva, G. V.; Litke, A. S.; Rudakova, A. V.; Ryabchuk, V. K.; Serpone, N. *Langmuir* **1998**, *14*, 5011.
- (14) Emeline, A. V.; Petrova, S. V.; Ryabchuk, V. K.; Serpone, N. *Chem. Mater.* **1998**, *10*, 3484.
- (15) Ryabchuk, V. K.; Basov, L. L.; Solonitzyn, Yu. P. *Usp. Photoniki, Iss. 0.7.*; Vilesov, Th. I., Ed.; LGU (Leningrad State University), **1980**, p 3.

- (16) Pichat, P.; Herrmann, J.-M.; Disdier, J.; Mozzanega, M.-N. *J. Phys. Chem.* **1979**, *83*, 3122.
- (17) Burukina, G. V.; Vitkovsky, G. E.; Ryabchuk, V. K. *Vestn. LGU 4; LGU (Leningrad State University)*, **1990**, *25*, 93.
- (18) Strekalovsky, V. N.; Polejaev, Yu. M.; Palguev, S. V. *Oxides with Extrinsic Disorder*; Nauka: Moscow, Russia; 1987.
- (19) Mikhailov, M. M.; Kuznetsov, N. Y. *Inorg. Mater.* **1988**, *24*, 656.
- (20) Mikhailov, M. M.; Dvoretzky, M. I.; Kuznetsov, N. Y. *Inorg. Mater.* **1984**, *20*, 449.
- (21) Emeline, A. V.; Rudakova, A. V.; Ryabchuk, V. K.; Serpone, N. *J. Phys. Chem. B* **1998**, *102*, 10906.
- (22) Basov, L. L.; Efimov, Yu. P.; Solonitsyn, Yu. P. *Uspechi Fotoniki, Iss. 4*; Vilesov Th. I., Ed.; LGU (Leningrad State University), **1974**, *12*.
- (23) Kotova, O. B. Ph.D. Thesis, Leningrad State University, Leningrad, Soviet Union, 1986.
- (24) Emeline, A. V.; Lobyntseva, E. V.; Ryabchuk, V. K.; Serpone, N. *J. Phys. Chem. B* **1999**, *103*, 1325.
- (25) Abdurazakov, A.; Antonov, V. A.; Arsen'ev, P. A.; Bagdasarov, H. S.; Kevorkov, A. N. *Inorg. Mater.* **1991**, *27*, 795.
- (26) Woosley, J. D.; Wood, C. *Phys. Rev. B*, **1980**, *22*, 1066.
- (27) Savihina, T. I.; Merilloo, I. A. *Trudi Inst-ta Fiziki AN ESSR, Tartu; Ed. Luschik, Ch. B.*, **1979**, *49*, 146.
- (28) Cain, L. S.; Pogatschnik, G. I.; Chen, Y. *Phys. Rev. B* **1988**, *37*, 2645.
- (29) Emeline, A. V.; Ryabchuk, V. K. *Fiz. Khim.* **1998**, *72*, 305.
- (30) White, G. S.; Jones, R. V.; Crawford, J. H., Jr. *J. Appl. Phys.* **1982**, *53*, 265.
- (31) Emeline, A. V.; Ryabchuk, V. K. *Fiz. Khim.* **1997**, *71*, 2085.
- (32) Schulman, J. H.; Compton, W. D. *Color Centers in Solids*. Pergamon Press: Oxford-London-New York-Paris, 1962.
- (33) Williams, R. T. *Semiconductors Insulators* **1978**, *3*, 251.
- (34) "Defects and Impurity Centers in Ionic Crystals: Optical and Magnetic Properties," Part 1. Special Issue, *J. Phys. Chem. Solids* **1990**, *51*, N. 7.
- (35) Bonch-Bruevich, V. L.; Kalashnikov, S. G. *Physics of Semiconductors*; Nauka: Moscow, Russia, 1990.
- (36) Siline, A. R.; Trukchin, A. N. *Point Defects and Elementary Excitation in Crystalline and Glass SiO<sub>2</sub>*; Zinatne Publishing House: Riga, 1985.
- (37) Pankove, J. I. *Optical Processes in Semiconductors*; Dover Publications: New York, 1971.
- (38) Bube, R. H. *Photoconductivity of Solids*; John Wiley & Sons: New York, 1960.
- (39) Aristov, Yu. I.; Parmon, V. N.; Zamaraev, K. I. *Khim. Fiz.* **1982**, *9*, 1233.
- (40) Serpone, N.; Khairutdinov, R. F. In *Semiconductor Nanoclusters – Physical, Chemical, and Catalytic Aspects*; Kamat, P.V.; Meisel, D.; Eds.; *Stud. Surf. Sci. Catal.* **1997**, *103*, 417.
- (41) Serpone, N.; Khairutdinov, R. F. *Prog. React. Kinet.* **1996**, *21*, 1.
- (42) Solonitzyn, Yu. P.; Prudnikov, I. M.; Yurkin, V. A. *Fiz. Khim.* **1980**, *57*, 2028.
- (43) Irradiation of a metal-oxide specimen produces active centers at the surface; if done in vacuo, the concentration of these centers is determined solely by their lifetime. In most metal oxides the lifetime is rather short, ca. 1–10 ms, such that once irradiation is stopped there will no longer be any surface active centers after a few tens of milliseconds because of their decay. In the case of ZnO, however, the lifetime of the active centers is at least a few days (perhaps because the energy levels of these centers are sufficiently deep that no thermal ionization takes place and because the probability of recombination through these centers is very low). Consequently, UV irradiation of ZnO in vacuo generates a maximal number of active centers under our conditions, and once irradiation is stopped introduction of O<sub>2</sub> (in the dark) leads to reaction with these centers and blocks these surface sites. If the specimen is now irradiated again, no new active sites can be generated and the reaction rate for the photostimulated adsorption of O<sub>2</sub> will consequently decrease sharply. Clearly the factor that contrasts ZnO with other metal oxides of Table 1 is the lifetime of the surface active centers produced by UV irradiation.
- (44) Che, M.; Tench, A. J. *Adv. Catal.* **1982**, *31*, 77.
- (45) The concentration of F color centers in eq 9 has a distinct meaning depending on whether it occurs in the numerator or in the denominator because of the dual role of F centers. In the numerator, [F] denotes the concentration of centers that absorb light (stage 5a), whereas [F] (or [V] = const [F]) in the denominator represents the concentration of F color centers that act as recombination centers. Consequently, under our proposed conditions, observation of a linear dependence of the reaction rate on the concentration of color centers infers that the efficiency of recombination  $k_{7a}$  through color centers must be comparable to the efficiency described by  $k_{6a}$  for electron trapping by anion vacancies in order to keep the concentration of color centers relatively low.
- (46) (a) Solonitzyn, Yu. P.; Kuzmin, G. N.; Shurigin, A. L.; Yurkin, V. M. *Kinet. Katal.* **1976**, *17*, 1267. (b) Basov, L. L.; Kuzmin, G. N.; Prudnikov, I. M.; Solonitzyn, Yu. P. *Usp. Photoniki, Iss. 6*; Vilesov, Th. I., Ed., LGU (Leningrad State University), **1977**, pp 82–120. (c) Andreev, N. S.; Koltel'nikov, V. A. *Kinet. Katal.* **1974**, *15*, 612. (d) Kondo, J.; Sakata, J.; Domen, K.; Marya, K.; Onisi, T. *J. Chem. Soc., Faraday Trans. 1* **1990**, *82*, 397.
- (47) Schrimmer, O. F. *J. Phys. C: Solid State Phys.* **1978**, *11*, L65.
- (48) Kuznetsov, V. N.; Skaletskaya, T. K.; Lisachenko, A. A. *Fiz. Khim.* **1980**, *54*, 2596.
- (49) Henderson, B.; Wertz, J. E. *Defects in Alkaline Earth Oxides with Application to Radiation Damage and Catalysis*; Taylor & Francis: London, 1977.
- (50) Crawford, J. H. *Semiconductors Insulators*, **1983**, *5*, 599.
- (51) In eq 23, it should be noted that  $\Delta[V]$  is proportional to  $\delta R$  and that  $[S^+]$ , which reflects the number of V centers, is proportional to  $\Delta P$ . The number of V centers given in the text was calculated using the following procedure: from the slope of the relationship between  $\Delta P$  and  $\delta R$  in Figure 7 we first estimate the number of molecules adsorbed using the ideal gas law and then we weight it by the extent of coloration  $\Delta R$  from Figure 5 of the UV-pre-irradiated specimen under the conditions of the experiment.
- (52) Llopis, J. *Phys. Status Solidi A* **1990**, *119*, 661.
- (53) Arsenov, P. A.; Bagdasarov, Kh. S.; Niklas, A.; Ryazantsev, A. D. *Phys. Status Solidi A* **1980**, *62*, 395.
- (54) Lorincz, A.; Puma, M.; James, F. J.; Crawford J. H. *J. Appl. Phys.* **1982**, *53*, 927.